Hindawi
International Journal of Polymer Science
Volume 2022, Article ID 1685064, 12 pages
https://doi.org/10.1155/2022/1685064

Research Article

Static and Dynamic Mechanical Properties of Recycled Concrete under Microwave Irradiation

Dandan Shi,[1] **Qingxuan Shi**,[2] **and Lei Yang**[3]

[1]*School of Civil Engineering, Xi'an Traffic Engineering Institute, 710000 Xi'an, China*
[2]*Xi'an University of Architecture and Technology, Key Laboratory of Structural Engineering and Earthquake Resistance, Ministry of Education, 710000 Xi'an, China*
[3]*SCEGC No.1 Construction Engineering Group Company Ltd, 710000 Xi'an, China*

Correspondence should be addressed to Dandan Shi; zje523_su@163.com

Received 26 June 2022; Revised 1 August 2022; Accepted 11 August 2022; Published 14 November 2022

Academic Editor: Yasir Nawab

The application of recycled concrete can alleviate environmental pollution and has great practical value. In this study, microwave irradiation technology is used to treat recycled concrete in order to obtain reinforced recycled coarse aggregate. Then, the quasi-static and dynamic mechanical properties of concrete (C), recycled concrete (RC), and recycled concrete irradiated by microwave (MRC) were studied, and the effect of the replacement rate of coarse aggregates on its mechanical properties was also studied. The results showed that the quasi-static compressive strength of MCR is higher than that of CR at all replacement rates. With the increase in the replacement rate, the quasi-static compressive strength of MCR decreases gradually, while the quasi-static compressive strength of CR decreases first and then increases, reaching the minimum value at 60%. The dynamic mechanical properties of CR and MCR all have an obvious strain rate effect. The dynamic increase factor (DIF) has an exponential relationship with the natural logarithm of the strain rate. The dynamic constitutive model of RC was established based on composite material mechanics and viscoelastic theory. The research content can provide guidance and basis for the study of mechanical properties and constitutive relationship of RC.

1. Introduction

Concrete is the most commonly used building material in the overall construction industry. According to the relevant reports, China's annual output of concrete is about 1.4 billion tons, accounting for about 48% of the world [1]. As the main material of concrete, the demand for coarse aggregate in engineering practice is likewise huge [2]. Excessive rock mining will destroy the ecological balance. The demolition of old buildings generates construction waste and occupies numerous land resources. Accordingly, it has brought enormous pollution to the environment [3].

Recycled concrete, also known as recycled aggregate concrete, is obtained by demolishing old buildings and then processing them through a specified process. Also, with a certain ratio through secondary mixing, the new concrete was formed in accordance with the recycled aggregate and natural aggregate [4]. To ensure the safety and stability of RC structures during service, it is essential to research the mechanical properties of this material. The development of RC is of great significance to environmental protection and resource recovery and reuse. On the basis of existing research, concrete recycling technology needs to be further promoted [5].

Many scholars have conducted experimental research and theoretical analysis on the mechanical properties of RC. Among them, S. Laserna and Montero [6] adopted four replacement rates to study the mechanical properties of crushed stone RC and pebble RC. Nobuaki et al. [7] researched the influence of water–cement ratio on the corrosion resistance of RC. Chen and Song [8] conducted compressive and flexural experimental studies on RC with different replacement rates and pointed out that there is a certain relationship between the content of recycled coarse aggregates and the mechanical properties of RC. Limbachiya et al. [9] selected two types of concrete, Portland cement and fly ash,

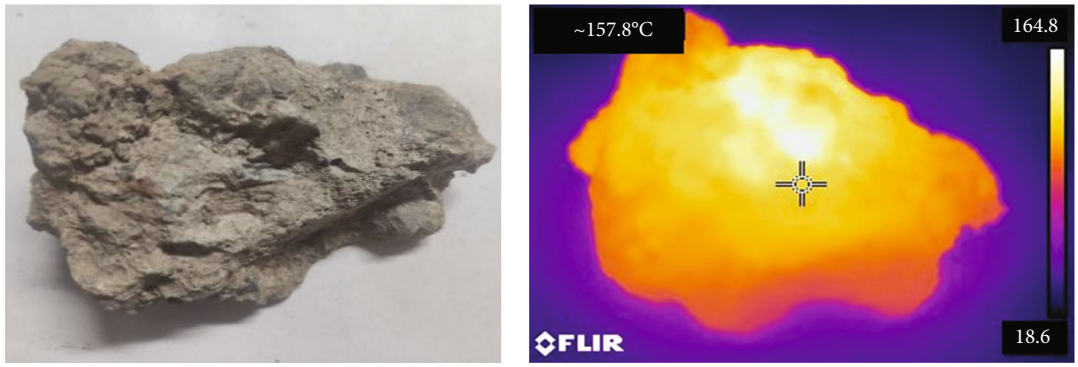

(a) (b)

Figure 1: Temperature distribution diagram after 8 min of microwave irradiation at 800 W: (a) concrete block; (b) temperature distribution.

but found that the recycled aggregate content had no obvious effect on the strength of RC. Overall, the performance of RC is different from that of ordinary concrete (OC), which is reflected in low strength, poor durability, and large dispersion. The main reason lies in the presence of old mortar on the surface of the coarse aggregate. The old mortar has low density, large porosity, and low strength. In the production of new concrete, poor contact between coarse aggregates and mortar has a significant impact on the mechanical properties of RC [10]. In order to make better use of coarse aggregates, Hu et al. [11] used four chemical reagents to strengthen the physical properties of recycled aggregates and studied its crushing and water absorption rate. Panduracngan [12] analyzed the primary factors affecting the bond strength of recycled aggregate concrete by using acid, heat, and mechanical treatments. Yang et al. [13] and Wang [14] accomplished the enhancement of recycled coarse aggregates by using different chemical reagents and adding mineral powder. By soaking recycled aggregate in PVP solution, Mansur et al. [15] and Wan et al. [16] studied the influence of chemical solution on the bonding properties of mortar and aggregates and pointed out that the mechanical properties of RC were significantly enhanced. Gjorv and Sakai [17], Ismail and Ramli [18], and Tam and Tam [19] removed the mortar on the surface of coarse aggregates by soaking and regenerating coarse aggregates in acid solutions of different types.

In addition, many scholars have improved the performance of concrete by adding composite fibers, steel fibers, and other materials to concrete. By studying the quasi-static mechanical properties of concrete with different fiber contents, the optimal fiber content can be obtained [20]. This method makes use of the excellent ductility of fiber materials and reduces cracks in concrete, which is a good recycling concrete utilization technology and has been widely used [21, 22].

There are many achievements in research on the performance of RC, mainly in quasi-statics. However, there is no unified understanding of the mechanical properties of RC with different replacement rates, which may be caused by the different types of recycled aggregates or the different mix ratios. In the process of service, in addition to the common quasi-static load, the RC structure will inevitably suffer from impact load, such as explosion, earthquake, or weapon attack [23]. In addition, as a concrete material, the dynamic strength of concrete has obviously improved under impact load [24]. There are few studies on the dynamic mechanical properties of RC, and the relationship between dynamic and static strength has not been established. The old mortar and ITZ on the surface of recycled coarse aggregate are the primary factors affecting the mechanical properties of RC. Most of the existing studies improve the physical and mechanical properties of RC using physical or chemical methods [25]. As a new technology, microwave irradiation technology is based on the principle that in the microwave heating process, the old mortar is severely dehydrated and becomes brittle, which can be better separated from the aggregate by mechanical means.

In this study, we conducted experimental research on the quasi-static and dynamic mechanical properties of C, RC, and MRC. Quasi-static compressive strength, dynamic compressive mechanical properties, and microscopic mechanism with different replacement rates are compared and investigated. Also, the dynamic constitutive model of RC is established. The research work has filled the gap in the research of dynamic mechanical behavior and dynamic constitutive relationship of RC and also provides guidance and basis for the safe service design of RC structures.

2. Experiment

2.1. Preparation of Recycled Coarse Aggregates by Microwave Irradiation. The concrete blocks with relatively complete crushing and medium mortar and aggregates were selected from the waste buildings, as shown in Figure 1(a). An EV 923KF6-NA microwave oven was used to irradiate the concrete blocks. The rated frequency was set to 2450 Hz and the rated voltage to 220 V. To achieve the purpose of separating aggregates from the mortar without causing serious loss of aggregate strength, the microwave irradiation time was set at 8 min and the microwave frequency was set at 800 W. Combined with related studies [26], the selection rate was statistically about 50%. An FLIR T400 infrared thermal imager was used to photograph the test blocks after microwave irradiation, and its temperature distribution is shown in Figure 1(b).

Table 1: 1 m^3 recycled concrete mixture.

Type	No.	Amount of concrete materials per cubic meter (kg/m^3)					
		Water cement ratio	Water	Cement	Sand	Natural aggregate	Recycled aggregate
C	C	0.5	185	370	637	1157	0
RC	RC-30	0.5	185	370	637	810	347
	RC-60					463	694
	RC-100					0	1157
MRC	MRC-30	0.5	185	370	637	810	347
	MRC-60					463	694
	MRC-100					0	1157

(a) (b)

Figure 2: Equipment for quasi-static and impact compression tests: (a) servo press tester; (b) split Hopkinson pressure bar.

Jaw crushers were used to crush the recycled aggregate. After sieving, the aggregate with a particle size of 5 ~ 20 mm was selected and prepared according to the continuous grading method. According to the experimental requirements, three different coarse aggregates were prepared, namely, natural coarse aggregate, recycled coarse aggregate, and microwave irradiation recycled coarse aggregate. Then, the coarse aggregate was put into the vacuum drying oven at 105°C for 24 h before use.

2.2. Specimen Preparation. The experiment used ordinary Portland cement, and the strength grade is 42.5R. The fine aggregate is the river sand. The water used is distilled water. The mix proportion of various types of RC is shown in Table 1. C represents concrete, RC represents unmodified recycled concrete, and MRC represents microwave irradiated recycled concrete.

After pouring, the concrete was preserved in a standard curing chamber for 28 days. The quasi-static specimen was processed as 100 × 100 × 100 mm cube, and the dynamic specimen size is 72 × 50 mm cylinder.

2.3. Test Equipment and Principles. The quasi-static compression test was carried out using a servo hydraulic press tester, as shown in Figure 2(a). The dynamic compressive test was conducted with a split Hopkinson pressure bar with a diameter of 76 mm, as shown in Figure 2(b). The length of the striker, incident bar, and transmission bar are 400 mm, 3200 mm, and 3200 mm, respectively. The bars are all alloy steel, the elastic modulus is 700 GPa, and the *P*-wave velocity is 5172 m/s.

The testing principle of the SHPB system is established based on the one-dimensional propagation theory of elastic wave and the assumption of stress uniformity [27]. In the process of data processing, the stress, strain, and strain rate of the specimen can be obtained by transforming the strain signals measured by the incident bar and transmission bar [28]. The calculation equations are:

$$\sigma(t) = \frac{E_c A_c}{2A_s}[\varepsilon_I(t) + \varepsilon_R(t) + \varepsilon_T(t)], \quad (1)$$

$$\varepsilon(t) = \frac{C_c}{l_s}\int_0^t [\varepsilon_I(t) - \varepsilon_R(t) - \varepsilon_T(t)]dt, \quad (2)$$

$$\dot{\varepsilon}(t) = \frac{C_c}{l_s}[\varepsilon_I(t) - \varepsilon_R(t) - \varepsilon_T(t)]. \quad (3)$$

Where $\varepsilon_I(t)$, $\varepsilon_R(t)$, and $\varepsilon_T(t)$ are the incident strain, reflection strain, and transmission strain, respectively; E_c, A_c, and C_c are the elastic modulus, cross-sectional area, and longitudinal wave velocity of the pressure bar, respectively; A_s and l_s are the cross-sectional area and the length of the specimen.

In order to study the effect of the replacement rate on strain rate sensitivity of RC, impact tests were carried out on each group of concrete with strain rates of 60 s^{-1}, 90 s^{-1}, and 120 s^{-1}, respectively. In order to eliminate the influence of specimen differences on the test results and ensure the accuracy of the test results, the quasi-static compression test

and impact compression test were repeated three times under each condition.

3. Result Analysis

3.1. Quasi-Static Compressive Strength. According to the quasi-static compression test, the quasi-static compressive strength of CR and MCR was obtained at different replacement rates, as shown in Figure 3.

Figure 3 shows that the quasi-static compressive strength of MCR is higher than that of CR at each replacement rate, and the difference between MCR and CR reaches the maximum value at the 60% replacement rate. With the increase in the replacement rate, the quasi-static compressive strength of MCR gradually decreases, while CR first decreases and then increases, reaching the minimum value at the 60% replacement rate. When the replacement rate is 30%, 60%, and 100%, the average quasi-static compressive strength of CR is 33.42 MPa, 25.82 MPa, and 27.87 MPa and that of MCR is 36.86 MPa, 35.29 MPa, and 31.96 MPa, respectively. The quasi-static compressive strength of MCR is increased by 10.29%, 36.67%, and 14.67% compared to CR when the replacement rate is 30%, 60%, and 100%, respectively. It can be observed that the quasi-static mechanical properties of RC are enhanced to a certain extent after microwave irradiation, and the growth rate is the highest when the replacement rate is 60%, and the improvement degrees of 30% and 100% are close.

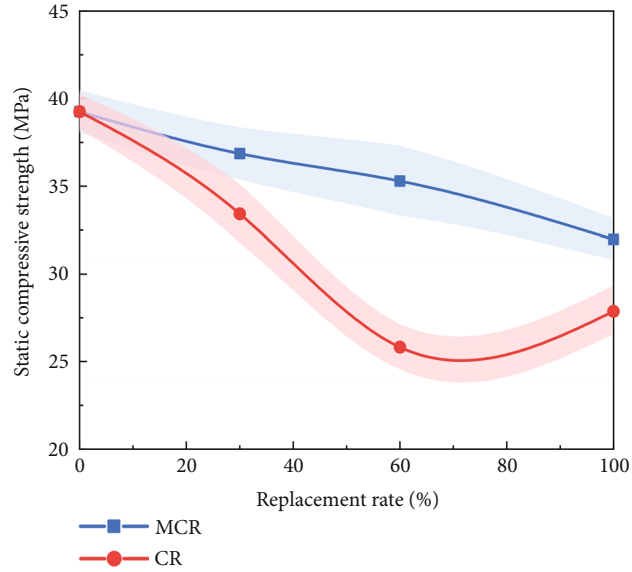

Figure 3: Quasi-static compressive strength of RC.

3.2. Dynamic Stress–Strain Curve. Dynamic compression tests were carried out on RC and MCR with different replacement rates, and the stress–strain curves obtained are shown in Figure 4.

In Figure 4, the dynamic stress–strain curves of RC and MRC under impact load can be roughly divided into three stages, namely, linear elastic stage, plastic hardening stage, and strain softening stage.

In the linear elastic stage, the stress of the specimen increases rapidly with the increase in strain. The two have a linear relationship and their slope remains basically unchanged. At this stage, the stress wave reaches a stable state after continuous reflection inside the specimen, and all absorbed and accumulated energy is elastic energy storage. Compared with the static stress curves, there is no compressive phase in the initial stage, which is because RC and MRC have strong brittleness and an obvious transverse inertia effect under impact load. At different strain rates, the slope remains basically unchanged at the same replacement rate, and there are certain differences in RC and MRC at different replacement rates.

In the plastic hardening stage, with the increase in strain, the rate of stress growth slows down, and the elastic energy storage of the specimen begins to release, which is used for the initiation and expansion of internal microcracks. Because of the high internal integrity and strong brittleness of the specimen, the internal crack extends rapidly under the action of load and the plastic hardening stage of C is not obvious. The specimen immediately reaches the peak strength and fails after reaching the elasticity limit, while the RC and MRC show an obvious plastic hardening stage.

In the strain softening stage, the stress decreases rapidly with the increase in strain, the crack in the specimen expands rapidly, and the specimen loses its bearing capacity and causes macroscopic failure. Because of the large dispersion of the specimen, it shows different downward trends.

It can be seen that the plastic hardening stage of RC and MRC accounts for more than that of C, which shows more obvious plasticity. With the replacement rate increase, the plasticity of the specimen becomes more obvious. At the same time, the slope of the linear elastic stage decreases significantly, and this stage is also defined as the dynamic elastic modulus of materials. Because elastic modulus does not have a strain rate effect, the dynamic elastic modulus of the specimen is related to the replacement rate of coarse aggregates and the type of concrete, but has nothing to do with the strain rate.

3.3. Dynamic Peak Stress. The relationship between the dynamic peak stress and the strain rate of RC and MRC is shown in Figure 5.

As the strain rate increases, the peak stresses of RC and MRC gradually increase, as shown in Figure 5, showing an obvious strain rate effect, and the two are in a linear relationship. At the same strain rate, the peak stress of the specimen has a certain error range, which is due to the uneven distribution of coarse aggregates in the specimen. The different degree of cementation between coarse aggregate and cementing material results in the difference in the internal structure. At strain rates of 60 ~ 120 s^{-1}, the strain rate effect of RC and MRC is primarily due to the interfacial transition zone (ITZ) interface damage and cracking at low strain rate, while the matrix and coarse aggregates of RC and MRC are damaged at a high strain rate. As a result, the strength of RC and MRC is enhanced, and the strain rate effect is obvious.

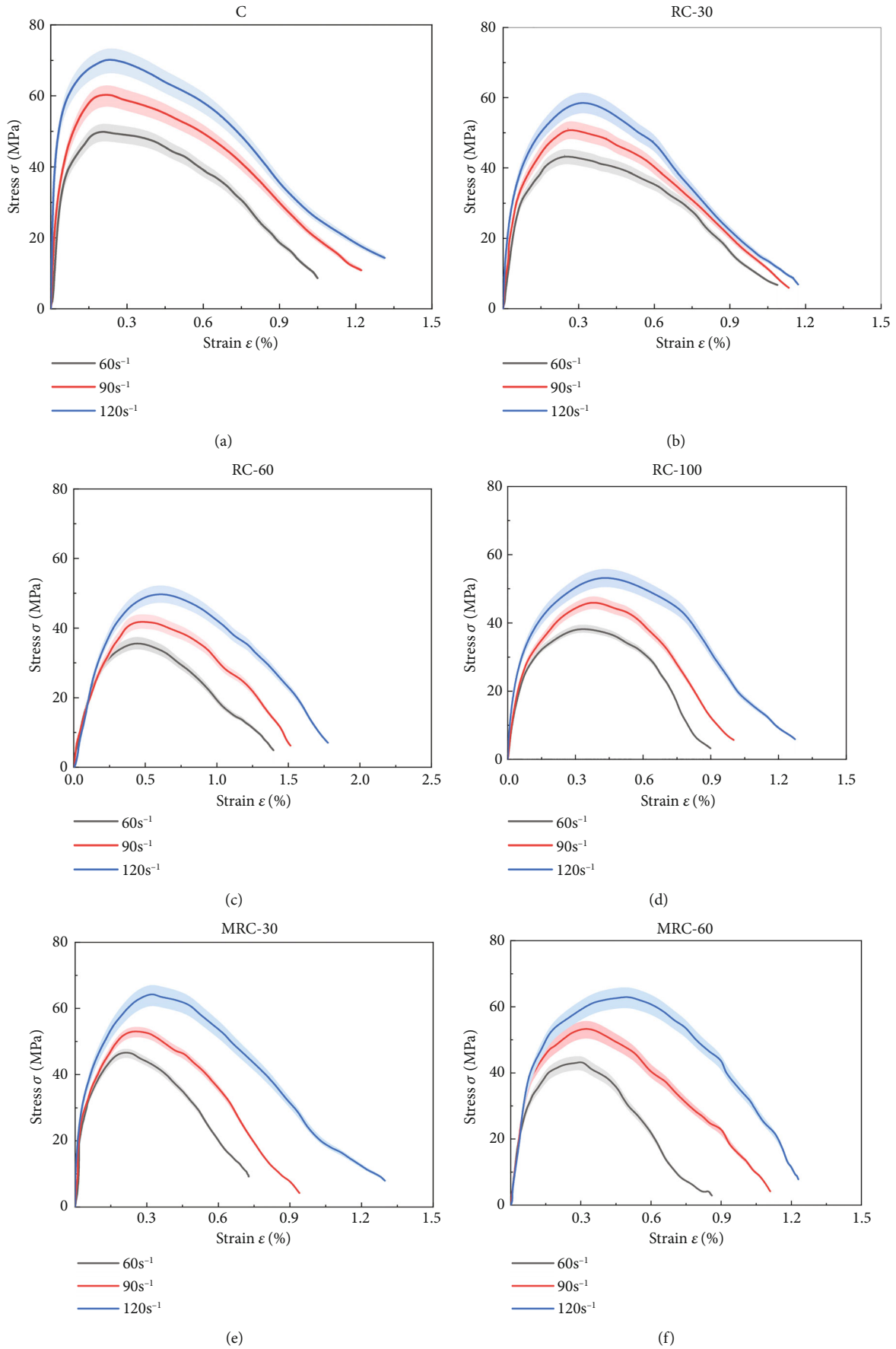

Figure 4: Continued.

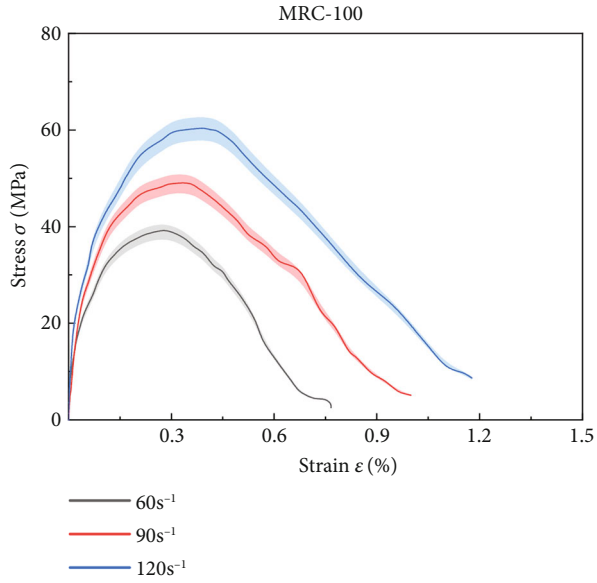

(g)

Figure 4: Dynamic stress–strain curves of RC and MRC: (a) C; (b) RC-30; (c) RC-60; (d) RC-100; (e) MRC-30; (f) MRC-60; (g) MRC-100.

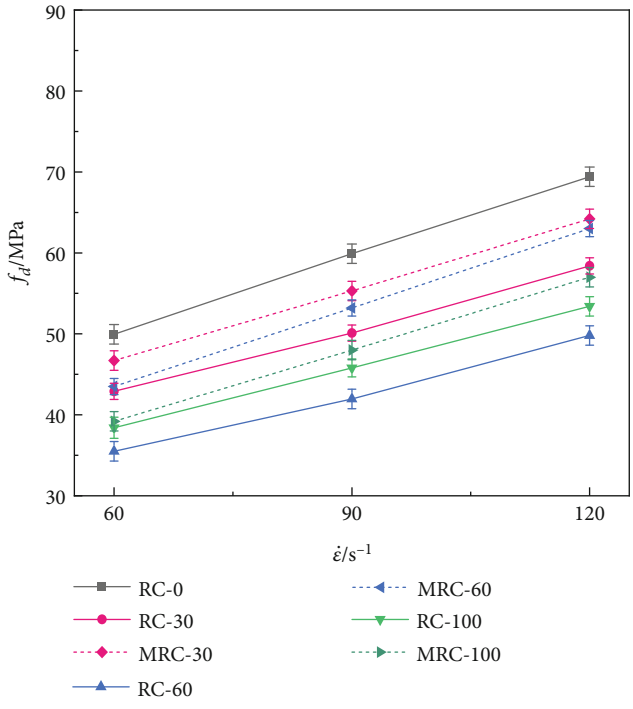

Figure 5: Relationship between the dynamic peak stress and strain rate.

Under the same strain rate, the peak stress of RC and MRC are both fewer than C. The sensitivity coefficients of C, RC-30, RC-60, and RC-100 were 0.32, 0.26, 0.24, and 0.25 and those of MRC-30, MRC-60, and MRC-100 were 0.29, 0.32, and 0.30. At the same replacement rate, the peak stress of MRC is higher than that of RC, and the rate sensitivity of MRC is slightly higher than RC. This is mainly because the old mortar on the coarse aggregate surface falls off under the action of microwave irradiation and the integrity of the specimen is improved. The ITZ needs to absorb more energy to crack when it is damaged, so it shows a higher rate sensitivity.

3.4. Dynamic Peak Strain. The peak strain of concrete can reflect the deformation characteristics of the material. The relationship between the dynamic peak strain and the strain rate of RC and MRC is shown in Figure 6.

Figure 6 shows that the peak strain of RC and MRC increases with the increase in the strain rate, showing an exponential relationship between them. Among them, the peak strain of RC-60 is the largest and the peak strain of C is the smallest. The peak strain of RC-30 and MRC-30, RC-100, and MRC-100 is close. The peak strain of MRC is slightly less than that of RC, indicating that the cementation between the recycled coarse aggregate and mortar matrix is reinforced after microwave irradiation. The elasticity of the material is enhanced while the plasticity is weakened. In addition, RC has many microdefects that will deform under impact load, thus increasing the strain value of the specimen.

3.5. Dynamic Increase Factor. The DIF is the ratio of the dynamic peak stress of the material to the quasi-static peak stress [29], and the calculation equation is as follows:

$$\mathrm{DIF}(\sigma) = \frac{f_\mathrm{d}}{f_\mathrm{s}}, \tag{4}$$

where f_d is the dynamic peak stress of concrete and f_s is the quasi-static peak stress.

The relationship between the DIF and the strain rate of RC and MRC is shown in Figure 7.

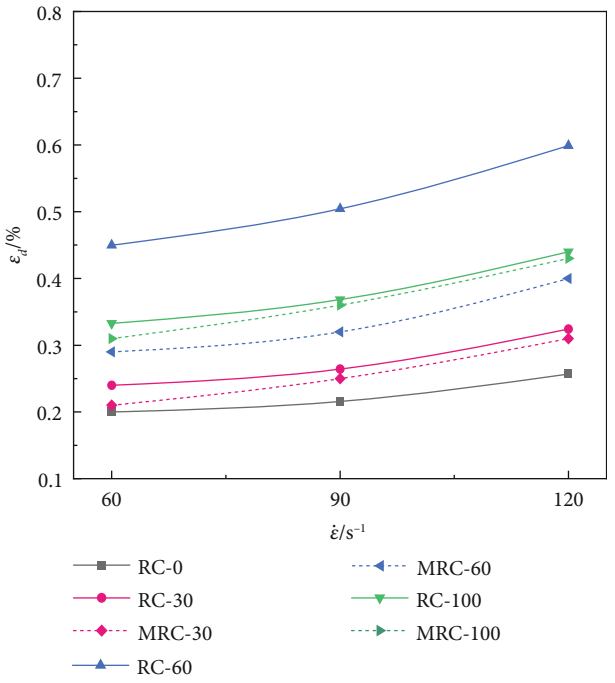

Figure 6: Relationship between dynamic peak strain and the strain rate.

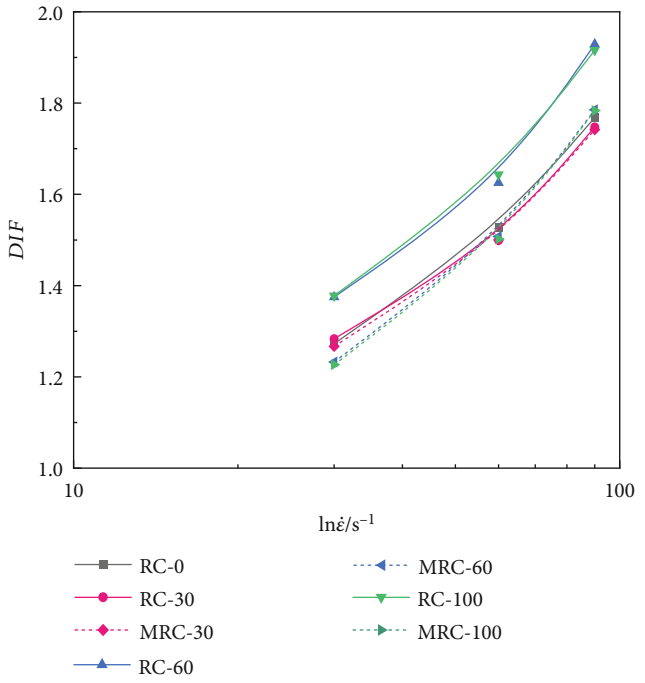

Figure 7: Relationship between the DIF and natural logarithm of the strain rate.

In Figure 7, DIF of RC and MRC increases with the increase of natural logarithm of strain rate, still showing an obvious strain rate effect and an exponential relationship between them.

Under impact load, the RC strain rate increases from 60 s^{-1} to 120 s^{-1}, and its DIF increases from 1.2 to 2. This is because when the impact load is small, the time for the microcracks in the specimen to expand to failure is sufficient. Under the action of stress waves, the primary microcracks are mainly propagated and destroyed, so the DIF is small. With the increase in the impact load, the microcracks in the specimen cannot expand sufficiently and the specimen is in a passive confining pressure state. At the same time, multiple cracks occur in the interior, which consumes a lot of energy, and the DIF continues to increase. With the further increase in the impact load, the energy absorbed by the specimen is used for the initiation and propagation of more secondary cracks; more cracks are developed in the matrix and aggregate, thus, the DIF increases continuously.

3.6. Microscopic Mechanism. A scanning electron microscope was used to observe the microstructure of the concrete aggregate and the mortar interface, as shown in Figure 8.

The cement mortar in C is comparatively compact, and a large number of hydration products and crystals are generated during the hydration process. The arrangement and distribution have no obvious regularity, and there are many microscopic pores exist in the cement mortar, as shown in Figure 8(a). The ITZ of C has a dense structure, and the bond between the mortar and aggregate is good. With a magnification of 2000 times, the gap between the ITZ is also small.

Figure 8(b) shows that there are a few hydration products in mortar in RC, indicating that the RC has completed part of the hydration process before production. The cohesiveness between the old mortar and the aggregate is poor, and the ITZ has larger pores and cracks. The reason may be that the recycled coarse aggregate is damaged during production by friction.

In Figure 8(c), there are still small cracks between the aggregate and the mortar in the ITZ of MRC. After microwave irradiation, a large number of old mortars were reduced, making the bond between new mortars and aggregate better. Nonetheless, microwave irradiation could not completely eliminate the old mortar on the aggregate surface, resulting in tiny cracks when combined with the new mortar.

According to SEM results, the internal microstructures of recycled coarse aggregate enhanced by microwave irradiation did not change much, and the number of microcracks on its surface and inside was not obvious. For recycling and reuse of waste concrete, the process of microwave-assisted aggregate picking can effectively separate the surface mortar. Also, the disturbance to the internal structure of coarse aggregate is small, so microwave-enhanced recycled aggregate technology has a certain application value.

3.7. Failure Mechanism. Under impact loading, the concrete failure degree increases with the increase in the strain rate, and its failure mechanism is shown in Figure 9.

Figure 9 shows that the strain rate effect of the specimen under impact load is a comprehensive reflection of the lateral inertia effect and the crack evolution effect. Under the impact load, the lateral effect is caused by the end friction

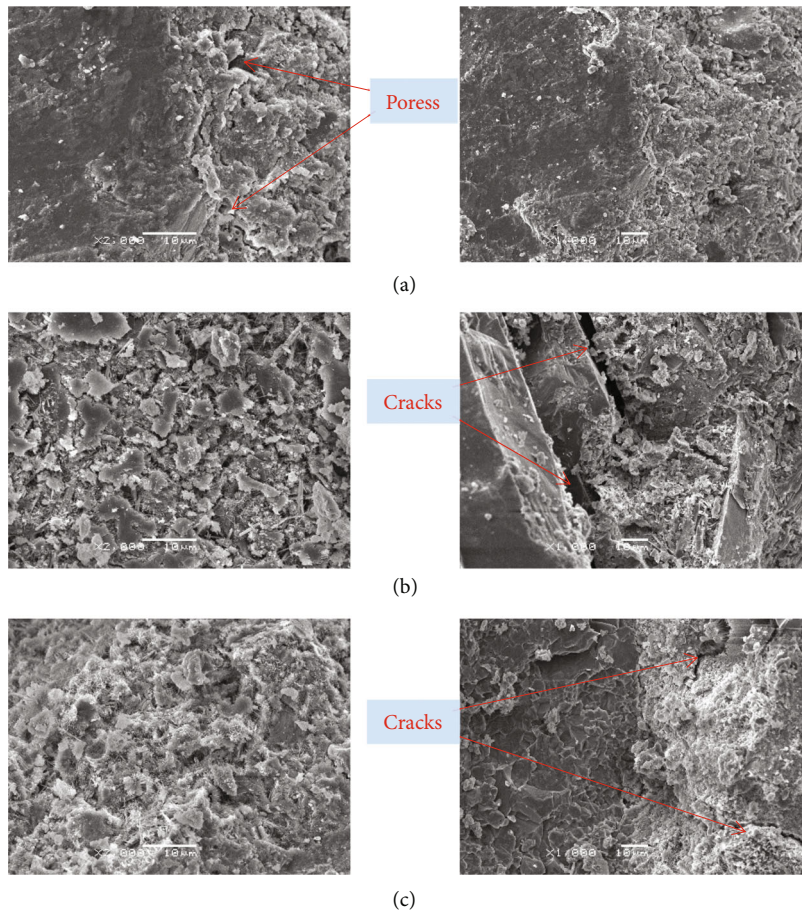

Figure 8: SEM images of the microstructure: (a) C; (b) RC; (c) MRC.

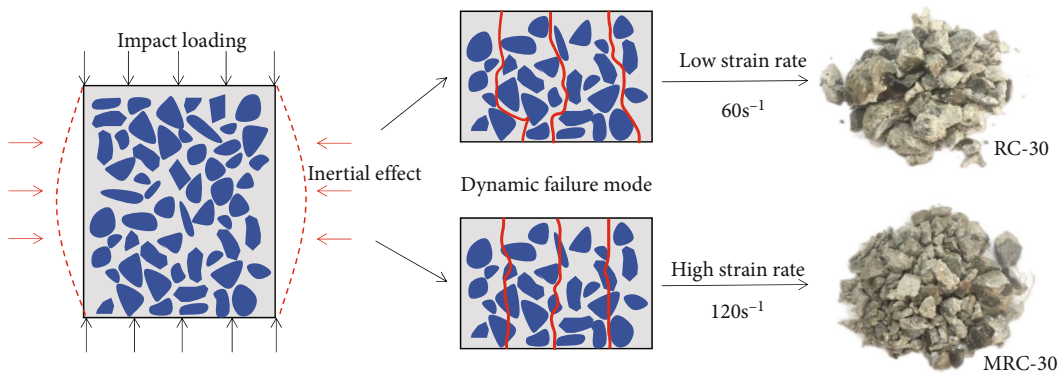

Figure 9: Dynamic failure mechanism.

and Poisson's ratio effect, which will cause the confining pressure to the outside of the specimen and will increase with the increase of the impact load. In the crack evolution effect, the matrix failure and ITZ debonding are the main failure factors at low strain rates. According to the principle of minimum energy consumption, the strength of the mortar and ITZ in RC is far less than the coarse aggregate, so the crack first expands and penetrates these two parts. Under the high strain rate, the energy absorbed by concrete increases greatly, reaching the energy needed for coarse aggregate to fracture and destroy, so the failure of coarse aggregate appears and the strength of concrete are obviously enhanced.

With the increase in the replacement rate, the compressive strength of RC decreases first and then increases. Combined with the microstructure and failure mechanism of

RC, there are mainly the following reasons: (1) Deterioration of mechanical properties of recycled coarse aggregate. In addition to the old mortar, there may be microcracks on the surface of the recycled aggregate. Compared with natural aggregates, it has lower strength, higher water absorption rate, and poor cementation. (2) The water absorption of recycled coarse aggregate is enhanced. In the concrete preparation process, the same water–cement ratio is utilized, but the water absorption rate of recycled aggregate is higher. With the continuous increase in the replacement rate, the recycled coarse aggregate absorbs more water, which decreases the water–cement ratio of the specimen, and thus, the strength of RC is enhanced to a certain extent.

Under the joint action of these two factors, if the influence of (1) is greater than that of (2), the strength of concrete is constantly reduced. On the contrary, if the influence of (1) is less than that of (2), the strength will be improved to a certain extent. Therefore, the strength of RC is lowest at the 60% replacement rate, but the strength of MRC decreases with the replacement rate. The reason is that the strengthening effect of microwave irradiation plays a certain role in the preparation of recycled coarse aggregate.

4. Dynamic Constitutive Model of RC

4.1. Establishment of the Constitutive Model. Concrete is a composite material composed of the mortar, coarse aggregate, and ITZ. According to the mechanics theory of composite materials, the constitutive relation of materials can be expressed as follows [30]:

$$\bar{\sigma} = \mathbf{L} : \bar{\varepsilon}, \tag{5}$$

$$\bar{\varepsilon} = \mathbf{M} : \bar{\sigma}, \tag{6}$$

where $\mathbf{L}$ and $\mathbf{M}$ are the stiffness matrix and the compliance matrix, respectively.

The RC is composed of N phase materials, and the sum of its volume fraction is 1. The corresponding stress and strain of each phase material are as follows [31]:

$$\bar{\varepsilon} = \sum_{r=0}^{N-1} C_r \bar{\varepsilon}^{(r)}, \tag{7}$$

$$\bar{\sigma} = \sum_{r=0}^{N-1} C_r \bar{\sigma}^{(r)}. \tag{8}$$

In RC, the volume proportion of ITZ is very small, and the stress in this part can be ignored. Thus, the stress of RC under impact load can be divided into two parts: one part is composed of the recycled coarse aggregate and the other part is the mortar. The existence of the ITZ can be equivalent to reducing the strength of the coarse aggregate, which can be represented by the reduction coefficient k. It can also be considered as the bond coefficient between the recycled coarse aggregate and the mortar.

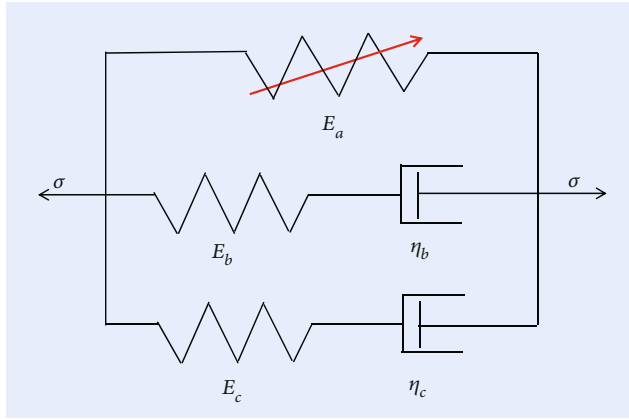

Figure 10: Z–W–T constitutive model.

The average stress of the recycled coarse aggregate is defined as $\bar{\sigma}_0$; then, the effective stress of RC can be expressed as follows:

$$\bar{\sigma}_0 = \sum_{k=0}^{k=1} k\sigma_0. \tag{9}$$

Assuming that the reduction coefficient of coarse aggregates and cement mortar in RC obeys Weibull distribution [32], the following equation can be obtained:

$$\bar{\sigma}_0 = \exp\left[-\left(\frac{\varepsilon}{\alpha}\right)^m\right]\sigma_0. \tag{10}$$

Then, the constitutive relation of RC is as follows:

$$\sigma = C_0 \exp\left[-\left(\frac{\varepsilon}{\alpha}\right)^m\right]\sigma_0 + C_1\bar{\sigma}_1, \tag{11}$$

where $\bar{\sigma}_1$ is the average stress of the cement mortar; C_0 and C_1 are the volume fractions of the coarse aggregate and the cement mortar, respectively.

It is considered that the coarse aggregate of RC is elastic under impact load before destruction, and its strength can be expressed as follows:

$$\sigma_0 = E_0\varepsilon, \tag{12}$$

where E_0 is the elastic modulus of the coarse aggregate.

The Z–W–T constitutive model is introduced to characterize the mechanical behavior of the mortar under impact load [33]. The Z–W–T constitutive model was established on the basis of the nonlinear viscoelastic constitutive model of homogeneous and isotropic materials in the one-dimensional condition, combined with a large number of impact tests of polymer viscoelastic materials [34]. The model is obtained by the parallel connection of two Maxwell bodies and a nonlinear spring, as shown in Figure 10.

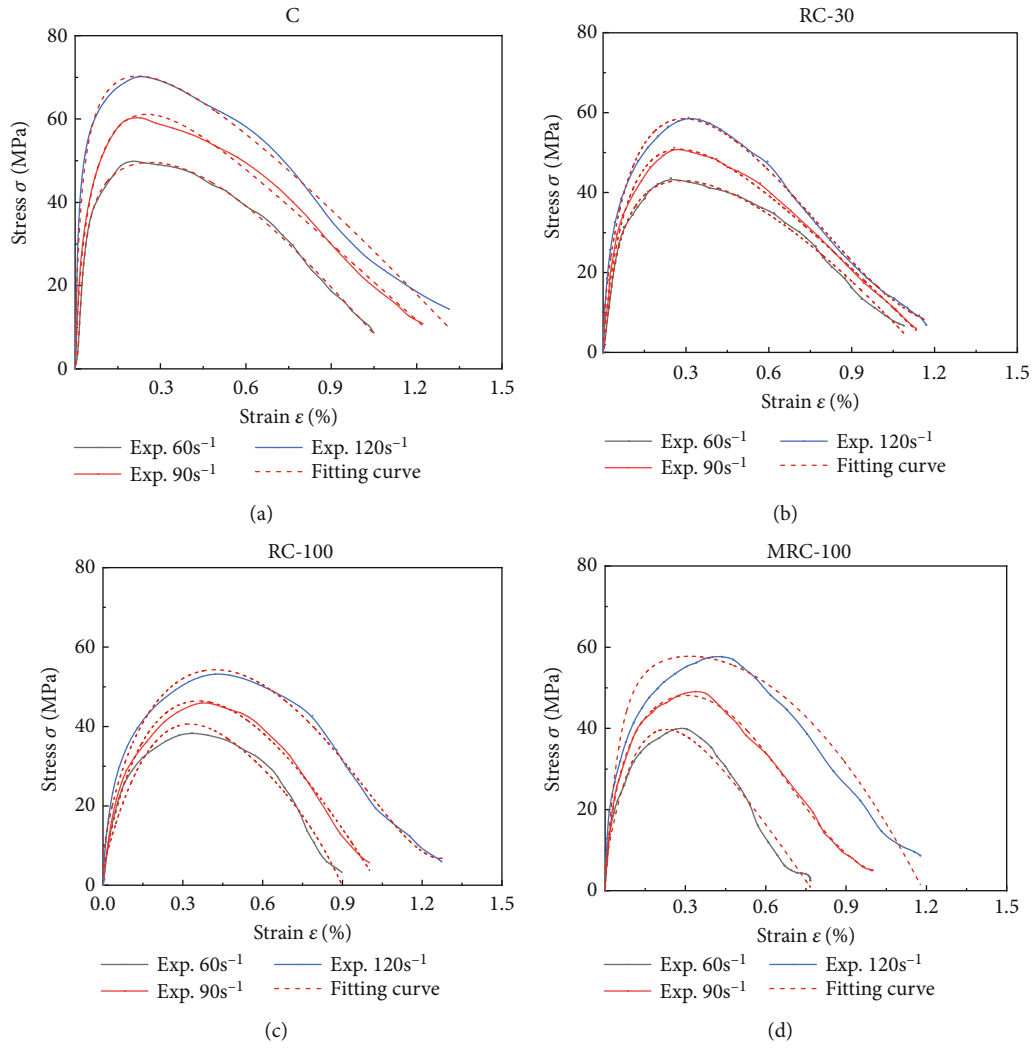

Figure 11: Validation of the constitutive equation: (a) C; (b) RC-30; (c) RC-100; and (d) MRC-100.

The constitutive equation of the Z-W-T model is as follows:

$$\sigma_1 = E_a\varepsilon + \alpha\varepsilon^2 + \beta\varepsilon^3 + E_b\int_0^t \dot{\varepsilon}\exp\left(-\frac{t-\tau}{\phi_b}\right)d\tau + E_c\int_0^t \dot{\varepsilon}\exp\left(-\frac{t-\tau}{\phi_c}\right)d\tau, \quad (13)$$

where E_a, A, and B are the elastic constant corresponding to the stress of the nonlinear elastic equilibrium response; E_b and ϕ_b are the elastic constants and relaxation time of the low-frequency Maxwell body, respectively; E_c and ϕ_c are the elastic constant and relaxation time of the high-frequency Maxwell body, respectively.

Integrating equation (13) and then substituting it into equation (11), the dynamic constitutive model of RC under impact load can be obtained:

$$\sigma = C_0\exp\left[-\left(\frac{\varepsilon}{\alpha}\right)^m\right]E_0\varepsilon + C_1\left\{E_a\varepsilon + A\varepsilon^2 + B\varepsilon^3 + \eta_b\dot{\varepsilon}\left[1-\exp\left(-\frac{E_b\varepsilon}{\eta_b\dot{\varepsilon}}\right)\right] + \eta_c\dot{\varepsilon}\left[1-\exp\left(-\frac{E_c\varepsilon}{\eta_c\dot{\varepsilon}}\right)\right]\right\}. \quad (14)$$

4.2. Validation of the Constitutive Model. According to the stress–strain curves of RC obtained from the dynamic compression test, the established constitutive model is verified, as shown in Figure 11. The corresponding value of the constitutive parameters is shown in Table 2.

Figure 11 shows that the constitutive curve is in good agreement with the test curve. The constitutive equation can well reflect the dynamic mechanical properties of RC under impact load, indicating that the dynamic constitutive

Table 2: Constitutive parameter values.

No.	α (10^{-4})	m	E_0 (GPa)	E_a (GPa)	A	B	n_b	E_b (GPa)	η_c	E_c (GPa)
C	17	0.93	40	5	$-1e-7 \sim -1e-6$	1	0.15 ~ 0.45	20	0.8	200
RC	1	0.12 ~ 0.18	40	5	$-1.5e-7 \sim -1.3e-7$	1	0.01 ~ 0.31	20	0.8	200
MRC	4	0.22 ~ 0.28	40	5	$-1.5e-7 \sim -1.3e-7$	1	0.15 ~ 0.35	20	0.8	200

model based on interface debonding damage can well characterize the impact mechanical constitutive relationship of RC. Although there are many unknown parameters in the constitutive equation in Table 2, the parameter values of RC with different strain rates and replacement rates are mostly fixed. Only α, m, A, and η_b change with the concrete type and the replacement rate.

5. Conclusions

In this study, the quasi-static and dynamic mechanical properties of C, RC and MRC are researched. The dynamic failure mechanism and microstructure are analyzed and its dynamic constitutive model based on composite material mechanics and the viscoelastic theory is established. The following conclusions can be drawn.

(1) The quasi-static compressive strength of MCR is higher than that of CR at the same replacement rate. With the increase in the replacement rate, the quasi-static compressive strength of MCR gradually decreases, while CR first decreases and then increases, reaching the minimum value at 60%.

(2) The dynamic mechanical properties of RC show an obvious strain rate effect. The peak stress has a linear relation with the strain rate, the peak strain has an exponential relation with strain rate, and the DIF has an exponential relation with the natural logarithm of the strain rate. After microwave irradiation, the number of pores in ITZ is reduced and the compactness of the internal structure is enhanced to a certain extent.

(3) Based on the constitutive theory of composite materials and the viscoelastic characteristics of RC under impact load, a dynamic constitutive model considering the bond performance of the coarse aggregate and mortar was established by introducing the Z-W-T model. The constitutive model is in good agreement with the experimental curve, which can better characterize the deformation and strength characteristics of recycled concrete under impact loading.

Data Availability

The data used to support the findings of this study are included within the article.

Conflicts of Interest

The authors declare that there are no conflicts of interest regarding the publication of this paper.

Acknowledgments

The work was supported by the Scientific Research Program Funded by the Education Department of Shaanxi Provincial Government (Program No. 22JK0449).

References

[1] A. Salesa, J. A. Perez-Benedicto, D. Colorado-Aranguren et al., "Physico - mechanical properties of multi - recycled concrete from precast concrete industry," *Journal of Cleaner Production*, vol. 141, pp. 248–255, 2017.

[2] C. Zhou and Z. Chen, "Mechanical properties of recycled concrete made with different types of coarse aggregate," *Construction & Building Materials*, vol. 134, pp. 497–506, 2017.

[3] M. X. Ma, V. W. Y. Tam, K. N. Le, and R. Osei-Kyei, "Factors affecting the price of recycled concrete: a critical review," *Journal of Building Engineering*, vol. 46, article 103743, 2022.

[4] M. B. Santos, J. D. Brito, and A. S. Silva, "A review on alkali-silica reaction evolution in recycled aggregate concrete," *Materials*, vol. 13, no. 11, p. 2625, 2020.

[5] A. Piccinali, A. Diotti, G. Plizzari, and S. Sorlini, "Impact of recycled aggregate on the mechanical and environmental properties of concrete: a review," *Materials*, vol. 15, no. 5, p. 1818, 2022.

[6] S. Laserna and J. Montero, "Influence of natural aggregates typology on recycled concrete strength properties," *Construction and Building Materials*, vol. 115, pp. 78–86, 2016.

[7] O. Nobuaki, M. Shin-Ichi, and Y. Wanchai, "Influence of recycled aggregate on interfacial transition zone, strength, Chloride penetration and carbonation of concrete," *Journal of Materials in Civil Engineering*, vol. 15, no. 5, pp. 443–451, 2003.

[8] H. X. Chen and X. Q. Song, "Experiment study on the strength dispersion of recycled aggregated concrete," *Journal of Xi'an University of Science and Technology*, vol. 41, no. 2, pp. 290–297, 2021.

[9] M. Limbachiya, M. S. Meddah, and Ouchagoury, "Use of recycled concrete aggregate in fly-ash concrete," *Construction and Building Materials*, vol. 27, no. 1, pp. 439–449, 2012.

[10] W. Ferdous, A. Manalo, R. Siddique et al., "Recycling of landfill wastes (tyres, plastics and glass) in construction—A review on global waste generation, performance, application and future opportunities," *Resources Conservation and Recycling*, vol. 173, article 105745, 2021.

[11] X. H. Hu, J. Xiao, H. P. Yang, C. F. Wu, and J. S. Zhang, "Experimental study on chemical strengthening of reclaimed coarse aggregate," *Journal of China & Foreign Highway*, vol. 39, no. 01, pp. 256–260, 2019.

[12] K. Pandurangan, A. Dayanithy, and S. Prakash, "Influence of treatment methods on the bond strength of recycled aggregate

concrete," *Construction and Building Materials*, vol. 120, pp. 212–221, 2016.

[13] N. Yang, C. G. Wang, and M. X. Zhao, "Research on intensifying technique of recycled aggregate," *New Building Materials*, vol. 38, no. 03, pp. 45–47, 2011.

[14] T. Wang, *Research on the Basic Strength Features of Recycled Concrete Aggregate and Recycled Concrete*, Shandong University of Science and Technology, Jinan, 2009.

[15] A. P. Mansur, D. B. Santos, and H. S. Mansur, "A microstructural approach to adherence mechanism of poly (vinyl alcohol) modified cement systems to ceramic tiles," *Cement and Concrete Research*, vol. 37, no. 2, pp. 270–282, 2007.

[16] H. W. Wan, J. L. Xu, Z. H. Shui, and J. Jiang, "Study on the structure and properties of interfacial transition zone (ITZ) of the regenerated concrete," *Journal of Wuhan University of Technology*, vol. 26, no. 11, pp. 29–32, 2004.

[17] O. E. Gjorv and K. Sakai, *Concrete Technology for a Sustainable Development in the 21st Century*, CRC Press, 1999.

[18] S. Ismail and M. Ramli, "Engineering properties of treated recycled concrete aggregate (RCA) for structural applications," *Construction and Building Materials*, vol. 44, pp. 464–476, 2013.

[19] V. W. Y. Tam and C. M. Tam, "Diversifying two-stage mixing approach (TSMA) for recycled aggregate concrete: $TSMA_s$ and $TSMA_{sc}$," *Construction and Building Materials*, vol. 22, no. 10, pp. 2068–2077, 2008.

[20] M. Umair, M. I. Khan, and Y. Nawab, "Green fiber-reinforced concrete composites," *Handbook of Nanomaterials and Nanocomposites for Energy and Environmental Applications*, pp. 1–32, 2020.

[21] M. I. Khan, M. Umair, K. Shaker, A. Basit, Y. Nawab, and M. Kashif, "Impact of waste fibers on the mechanical performance of concrete composites," *The Journal of The Textile Institute*, vol. 111, no. 11, pp. 1632–1640, 2020.

[22] M. Ahmadi, S. Farzin, A. Hassani, and M. Motamedi, "Mechanical properties of the concrete containing recycled fibers and aggregates," *Construction and Building Materials*, vol. 144, pp. 392–398, 2017.

[23] Z. Tang, W. Li, V. W. Y. Tam, and Z. Luo, "Investigation on dynamic mechanical properties of fly ash/slag-based geopolymeric recycled aggregate concrete," *Composites Part B: Engineering*, vol. 185, article 107776, 2020.

[24] J. Guo, Q. Chen, W. Chen, and J. Cai, "Tests and numerical studies on strain-rate effect on compressive strength of recycled aggregate concrete," *Journal of Materials in Civil Engineering*, vol. 31, no. 11, p. 04019281, 2019.

[25] Á. Salesa, J. Á. Pérez-Benedicto, L. M. Esteban, R. Vicente-Vas, and M. Orna-Carmona, "Physico-mechanical properties of multi-recycled self-compacting concrete prepared with precast concrete rejects," *Construction and Building Materials*, vol. 153, pp. 364–373, 2017.

[26] Z. Pengju, W. Wei, S. Zhushan, and Q. Rujia, "Effect of moisture on concrete damage and aggregate recycling under microwave irradiation," *Journal of Building Engineering*, vol. 46, article 103741, 2022.

[27] E. A. Flores-Johnson and Q. M. Li, "Structural effects on compressive strength enhancement of concrete-like materials in a split Hopkinson pressure bar test," *International Journal of Impact Engineering*, vol. 109, pp. 408–418, 2017.

[28] Y. Al-Salloum, T. Almusallam, S. M. Ibrahim, H. Abbas, and S. Alsayed, "Rate dependent behavior and modeling of concrete based on SHPB experiments," *Cement & Concrete Composites*, vol. 55, pp. 34–44, 2015.

[29] S. J. Zhao and Q. Zhang, "Effect of silica fume in concrete on mechanical properties and dynamic behaviors under impact loading," *Materials*, vol. 12, no. 19, p. 3263, 2019.

[30] S. Oller, E. Onate, J. Miquel, and S. Botello, "A plastic damage constitutive model for composite materials," *International Journal of Solids & Structures*, vol. 33, no. 17, pp. 2501–2518, 1996.

[31] A. D. Jefferson and T. Bennett, "A model for cementitious composite materials based on micro-mechanical solutions and damage-contact theory," *Computers & Structures*, vol. 88, no. 23–24, pp. 1361–1366, 2010.

[32] X. M. Hou, S. J. Cao, Q. Rong, W. Zheng, and G. Li, "Effects of steel fiber and strain rate on the dynamic compressive stress-strain relationship in reactive powder concrete," *Construction and Building Materials*, vol. 170, pp. 570–581, 2018.

[33] H. Zhang, B. Wang, A. Y. Xie, and Y. Qi, "Experimental study on dynamic mechanical properties and constitutive model of basalt fiber reinforced concrete," *Construction & Building Materials*, vol. 152, pp. 154–167, 2017.

[34] H. Tan, Y. Huang, C. Liu, and H. Geubellec, "The Mori-Tanaka method for composite materials with nonlinear interface debonding," *International Journal of Plasticity*, vol. 21, no. 10, pp. 1890–1918, 2005.